Aryl piperazine and pyrrolidine as antimalarial agents.
Synthesis and investigation of structure-activity relationships

Adela Mendoza[a], Silvia Pérez-Silanes[a] Miguel Quiliano[b], Adriana Pabón[c], , Germán González[b], Giovanny Garavito[d], Mirko Zimic[b], Abrahm Vaisberg[b], Ignacio Aldana[a], Antonio Monge[a], Eric Deharo [e,f]

[a]*Unidad en Investigación y Desarrollo de Medicamentos, Centro de Investigación en Farmacobiología Aplicada (CIFA), University of Navarra, Pamplona, Spain.*
[b]*Laboratorios de Investigación y Desarrollo, Facultad de Ciencias y Filosofía, Universidad Peruana Cayetano Heredia (UPCH), Av. Honorio Delgado 430, SMP, Lima, Peru.*
[c]*Grupo Malaria, Universidad de Antioquia, Medellín Colombia.*
[d] *Departamento de Farmacia, Facultad de Ciencias, Universidad Nacional de Colombia (DFUNC), Carrera 30 45-03, Bogotá D.C. Colombia*
[e]*Université de Toulouse; UPS; UMR 152 (Laboratoire de pharmacochimie des substances naturelles et pharmacophores redox), 118, rte de Narbonne, F-31062 Toulouse cedex 9, France.*
[f]*IRD, UMR-152, Mission IRD casilla 18-1209 Lima, Peru.*

** Corresponding author. Address: Mission IRD casilla 18-1209 Lima 18, Peru.*
Fax + 51 1 441 32 23 22.
E-mail address: eric.deharo@ird.fr (E. Deharo)

Abstract

Piperazine and pyrrolidine derivatives were synthesized and evaluated for their capacity to inhibit the growth of *Plasmodium falciparum* chloroquine-resistant (FCR-3) strain in culture. The combined presence of a hydroxyl group, a propane chain and a fluor were shown to be crucial for the antiplasmodial activity. Five compounds of the aryl-alcohol series inhibited 50% of parasite growth at doses ≤ 10 µM. The most active compound *1-(4-fluoronaphthyl)-3-[4-(4-nitro-2-trifluoromethylphenyl)piperazin-1-yl]propan-1-ol* was almost 20 to 40 times more active on *Plasmodium falciparum* (IC50: 0.5 µM) than on tumorogenic and non tumorogenic cells. Calculated physicochemical parameters showed a good potential for intestinal absorption, but due to difficulty in being solubilised prior to oral administration, it was weakly active against *Plasmodium berghei* infected mice (ED50: 35%). *In silico* molecular docking study and molecular electrostatic potential calculation revealed that this compound bound to the active site of *Plasmodium* plasmepsin II enzyme.

Index Descriptors and Keywords: Piperazine; Pyrrolidine; Antiplasmodial; *Plasmodium;* antimalarial agents; docking studies.

1. Introduction

In spite of huge efforts to fight malaria for the last 50 years, this plague is still a major health problem in developing countries with around 500 million cases and 3 million deaths every year (WHO, 2008). The emergence of resistance to almost all available treatments lead to an alarming situation in endemic areas. New therapeutic alternatives are thus urgently needed.

Recently, hydroxyethylpiperazine derivatives have been shown to be active against chloroquine resistant strain of *Plasmodium falciparum in vitro* with low toxicity against murine monocyte/macrophage cells (J774) (Cunico et al. 2009a,b). Computational studies also showed that piperazine derivatives could target *Plasmodium* plasmepsin II enzyme (Cunico et al., 2009a). This enzyme, that recently caused much interest, is involved in the initial steps of the hemoglobin degradation (see Ersmark et al., 2006 for review), which is a critical issue in the intra-erythrocytic cycle of the parasite, taking place inside the food vacuole. Thus, in the search for inexpensive alternative medicines, we described herein the synthesis, antiplasmodial activity and physicochemical parameters of piperazine and pyrrolidine derivatives. These compounds were tested against *P. falciparum* infected red blood cells (for antimalarial properties) and on murine peritoneal macrophages (for toxicity against non proliferative cells). The most active compound was also screened for antimalarial activity *in vivo* on *P. berghei* infected mice, for cytotoxicity against a panel of tumorogenic and non tumorogenic cells. Finally, it was submitted to a docking analysis with the active site of *Plasmodium* plasmepsin II enzyme.

2. Materials and methods

2.1. Chemicals and instruments

Chemicals reagents were purchased from E. Merck (Darmstadt, Germany), Scharlau (F.E.R.O.S.A., Barcelona, Spain), Panreac Química S.A. (Montcada i Reixac, Barcelona, Spain), Sigma-Aldrich Química, S.A., (Alcobendas, Madrid), Acros Organics (Janssen Pharmaceuticalaan 3a, 2440 Geel, België) and Lancaster (Bischheim-Strasbourg, France).

All of the synthesized compounds were chemically characterized by thin layer chromatography (TLC), melting point (m.p.), infrared (IR) and nuclear magnetic resonance (^{1}H-NMR) spectra as well as by elemental microanalysis.

^{1}H NMR spectra were recorded on a Bruker 400 Ultrashield (400 MHz) (Rheinstetten, Germany), using TMS as internal standard and chloroform ($CDCl_3$) or dimethyl sulfoxide- d_6 (DMSO-d_6) as solvents; the chemical shifts are reported in ppm (δ), and coupling constant (J) values are given in Hertz (Hz). Signal multiplicities are represented by: s (singlet), bs (broad singlet), d (doublet), t (triplet), q (quadruplet), d-d (double doublet), d-d-d (double double doblet) and m (multiplet). The IR spectra were performed on Thermo Nicolet FT-IR Nexus Euro (Madison, USA) using KBr pellets; the frequencies are expressed in cm^{-1}. Elemental microanalyses were obtained on an Elemental Analyzer (LECO CHN-900, Michigan, USA) from vacuum-dried samples. The analytical results for C, H, and N were within ± 0.4 of the theoretical values.

Alugram SIL G/UV254 (Layer: 0.2 mm) (Macherey-Nagel, Germany) was used for thin layer chromatography and silica gel 60 (0.040-0.063 mm and 0.063-0.200 nm) for column flash chromatography (Merck).

Some ketones and hydroxyls were purified by flash chromatography with binary gradient of dichloromethane (synthesis grade, SDS- Carlo Erba Reactifs, France) with methanol (Panreac Química S.A.) until 99:1 and a UV variable dual – wavelength detection. The chromatography was developed in the CombiFlash® RF (Teledyne Isco, Inc., Lincoln, USA), with CH_2Cl_2 - methanol as solvents and a normal phase of 12 gram Flash Column (RediSep® Rf Columns by Teledyne Isco, Inc., USA).

2.2. Synthesis of piperazine derivatives

Methods for the synthesis of compounds **(1- 14)** are presented in fig.1-3. The synthesis of some of the tested compounds has been published previously (Pérez Silanes et al., 2009).

The 1- (3- benzo[*b*]thiophenyl)-3-chloropropan -1-one **(I)** precursor was synthesized by a Friedel-Craft acylation as described (Oficialdegui et al., 2000). The 2- bromo-2´-acetonaphthone **(II)** was commercially available. Ketones **(1-3)** were synthesized by nucleophilic attack of the corresponding arylamine **(IV)** or **(V)** to **(I)** or **(II)** via S_N2 mechanism (fig.1).

The ketone intermediates **(4-6)** were prepared by condensation of the corresponding acetophenone **(III)** (commercially available) with the different aryl amines **(IV)** and **(V)** via Mannich reaction (fig.1).

2-nitro-4-trifluromethyl phenyl piperazine **(V)** was commercially available. The other aryl amine (**IV)** was synthesized using the corresponding BOC-amines and 4-nitro-2-trifluoromethylphenyl as aryl fluorides by an Ar-S_N reaction via Meisenheimer complex

(Bruckner, 2002) and posterior removal of the BOC-group with HCl and acetic acid (fig.2).

Finally, all the hydroxyl derivatives (**7-13)** were obtained by reduction of the corresponding carbonyl group with $NaBH_4$ in methanol (fig.1). The oxime **(14)** was obtained by condensation of the corresponding carbonyl group with hydroxylamine hydrochloride in ethanol (fig.3).

2.2.1. General method for the synthesis of protected aryl amines (VI)

A mixture of the 2-fluoro-4-nitrobenzo-trifluoride (1 eq), the protected amine **(VI)** (1.2 eq), K_2CO_3 (1.5 eq) and CH_3CN (30mL) was heated at reflux for 24 hours. The solvent was removed under reduced pressure; the residue was dissolved in CH_2Cl_2 (50mL) and washed with water (3x30mL). The organic phase was dried with anhydrous Na_2SO_4 and filtered. After evaporating to dryness under reduced pressure, the residue was precipitated and washed by adding diethyl ether or petroleum ether, affording the desired protected aryl amine (**VII).**

2.2.2. General method for the deprotection of amines (IV)

The protected amine (**VII)** was dissolved in 40 mL of a solution of HCl/AcH (1:1) with stirring for 2 hours at room temperature. The solvent was removed under reduced pressure and the compound was dissolved in water. The aqueous solution was basified with NaOH 2M to basic pH and stirred for 1 hour. Then the product was extracted with CH_2Cl_2. The organic phase was dried with anhydrous Na_2SO_4 and filtered. After evaporating to dryness under reduced pressure, the crude was purified by column chromatography (SP: silica gel), eluting with $CH_2Cl_2(NH_3)$/methanol 99:1 (v/v) affording the desired deprotected amine **(IV).**

*2.2.3. General method for the synthesis of ketones (***1-3***)*

A mixture of 1-(benzo[*b*]thiophen-3-yl)-3-chloropropan-1-one (**I**) (1 eq) or 2-bromo-2´-acetonaphthone **(II**), the arylamine (**IV**) or **(V)** (1.2 eq) and K_2CO_3 (1.5 eq) was stirred in THF for 72 hours at room temperature. The solvent was removed under reduced pressure and the residue was dissolved in CH_2Cl_2 (40 mL) and washed with water (3x30mL). After evaporating to dryness under reduced pressure the residue was purified by column chromatography (SP: silica gel), eluting with CH_2Cl_2/methanol 99:1 (v/v). In some cases the compound has been purified by preparative chromatography (SP: silica gel), eluting with CH_2Cl_2/methanol 97:3 (v/v). In the cases in which the

hydrochloride salt was prepared, the process consisted in adding a hydrogen chloride ethereal solution to a dichloromethane solution of the compound.

*2.2.4. General method for the synthesis of ketones (***4-6***)*

A mixture of the appropriated substituted acetophenone (**III**) (1 eq), arylamine (**IV)** or **(V)** (1 eq), dioxolane (1.4%) and concentrated HCl (1 mL) was heated at reflux. Then add water (50 mL) and the product was extracted with CH_2Cl_2. The organic phase was dried with anhydrous Na_2SO_4, filtered and after evaporating to dryness under reduced pressure. The residue was purified by column chromatography (SP: silica gel), eluting with CH_2Cl_2/methanol 95:5 (v/v) or Flash Chromatography eluting with CH_2Cl_2/methanol 99:1 (v/v). In other cases in which the hydrochloride salt was prepared, the process consisted in adding a hydrogen chloride ethereal solution to the compound stirring and washes with diethyl ether.

*2.2.5. General method for preparation of hydroxyl derivatives (***7-13***)*

Sodium borhydride (3 eq) was added little by little to a pre-cooled suspension (0ºC, 5 min) of the corresponding ketone (1eq) in methanol over a period of 30-60 minutes. The solvent was removed under reduced pressure and the residue dissolved in dichloromethane (40 mL) was washed with water (3x30 mL). The organic phase was dried with anhydrous Na_2SO_4 and filtered. After evaporating the solvent to dryness under reduced pressure, the compound was purified by column chromatography (SP: silica gel), eluting with CH_2Cl_2/methanol 99:1 (v/v), by preparative chromatography (SP: silica gel), eluting with CH_2Cl_2/methanol 97:3 (v/v), Flash Chromatography eluting with CH_2Cl_2/methanol 99:1 (v/v) or preparing the hydrochloride.

*2.2.6. General method for preparation of oxime derivative (***14***)*

The ketone **(5)** (1eq) and hydroxylamine chlorhydrate (5.5eq) in ethanol was heated at reflux during 90 minutes. Then solution was basified with NaOH in ethanol-water to pH 9 and heated reflux during 30 minutes more. Then add water (50 mL) and the product was extracted with ethyl acetate. The organic phase was dried with anhydrous Na_2SO_4, filtered and after evaporating to dryness under reduced pressure. The compound was purified washing with CH_2Cl_2/ diethyl ether.

2.3. Structural data

1-(benzo[b]thiophen-3-yl)-3-[4-(4-nitro-2-trifluoromethylphenyl)piperazin-1-

*yl]propan-1-one (Compound **1**)* (13 % Yield). Mp 140-141ºC. ^{1}H NMR (400 MHz, $CDCl_3$): δ 2.76-2.77 (m, 4H, **H_2** + **H_6** piperazine); 3.02 (q, 2H, CO-CH_2-C**H_2**); 3.19-3.21 (t, 4H, **H_3** + **H_5** piperazine); 3.27-3.30 (q, 1H, CO-C**H_2**-CH_2); 7.29 (d-d, 1H, **$H_{6'}$** phenyl, $J_{6',5'}$ = 9.4 Hz, $J_{6',3'}$ = 2.5 Hz); 7.46 (t, 1H, **H_6** benzothiophenyl, $J_{6,5}$ = 8.0 Hz); 7.52 (t, 1H, **H_5** benzothiophenyl, $J_{5,4}$ = 8.1 Hz); 7.90 (d, 1H, **H_4** benzothiophenyl, $J_{4,5}$ = 8.0 Hz); 8.33-8.36 (m, 2H, **$H_{5'}$** phenyl + **H_7** benzothiophenyl); 8.53 (s, 1H, **H_2** benzothiophenyl); 8.78 (d, 1H, **$H_{3'}$** phenyl) ppm. Anal ($C_{22}H_{20}N_3F_3O_3S$) C, H, N.

*1-(2-naphthyl)-2-[4-(4-nitro-2-trifluoromethylphenyl)piperazin-1-yl] ethan-1-one (Compound **2**)* (13% Yield) Mp 167–168ºC. ^{1}H NMR (400 MHz, $CDCl_3$): δ 3.09 (bs, 4H, H_2+H_6 piperazine); 3.36 (bs, 4H, H_3+H_5 piperazine); 4.28 (bs, 2H, $COCH_2$); 7.39 (d, 1H, $H_{6'}$ phenyl, $J_{6',5'}$ = 8.8 Hz); 7.60 (d-d-d, 1H, H_6 naphthyl); 7.66 (d-d-d, 1H, H_7 naphthyl); 7.92 (d, 1H, H_3 naphthyl, $J_{3,4}$ = 8.1 Hz); 7.94 (d, 1H, $H_{5'}$ phenyl, $J_{5',6'}$ = 8.9 Hz); 8.00 (d, 1H, H_4 naphthyl, $J_{4,3}$ = 8.1 Hz); 8.05 (d-d, 1H, H_5 naphthyl, $J_{5,6}$ = 8.5 Hz, $J_{5,7}$ = 1.2 Hz); 8.37 (d-d, 1H, H_8 naphthyl, $J_{8,7}$ = 9.0 Hz, $J_{8,6}$ = 1.9 Hz); 8.56 (bs, 2H, H_1 naphthyl+ $H_{3'}$ phenyl) ppm. Anal ($C_{23}H_{20}N_3F_3O_3$) C, H, N.

*1-(2-naphthyl)-2-[4-(2-nitro-4-trifluoromethylphenyl)piperazin-1-yl] ethan-1-one (Compound **3**)* (60% Yield) Mp 106–107ºC. ^{1}H NMR (400 MHz, $CDCl_3$): δ 2.90 (t, 4H, **H_2**+**H_6** piperazine); 3.31 (t, 4H, **H_3**+**H_5** piperazine); 4.10 (bs, 2H, CO-**CH_2**); 7.21 (d, 1H, **$H_{6'}$** phenyl, $J_{6',5'}$ = 8.6 Hz); 7.60 (d-d, 1H, **H_7** naphthyl, $J_{7,5}$ = 8,4 Hz, $J_{7,8}$ = 8.5 Hz); 7.64 (d-d, 1H, **H_4** naphthyl, $J_{4,3}$ = 8.1 Hz, $J_{4,5}$ = 1.4 Hz); 7.69 (ddd, 1H, **H_6** naphthyl); 7.91 (d, 1H, **H_5** naphthyl, $J_{5,6}$ = 9.5 Hz); 7.94 (d, 1H, **H_8** naphthyl, $J_{8,7}$ = 8.4 Hz); 8.00 (d, 1H, **H_3** naphthyl, $J_{3,4}$ = 8.1 Hz); 8.06 (dd, 1H, **$H_{5'}$** phenyl, $J_{5',6'}$ = 8.6 Hz, $J_{5',3'}$ = 1.6 Hz); 8.09 (d, 1H, **$H_{3'}$** phenyl, $J_{3',5'}$ = 1.6 Hz); 8.56 (bs, 1H, **H_1** naphthyl) ppm. Anal ($C_{23}H_{20}N_3F_3O_3$) C, H, N.

*Hydrochloride of 1-(2-naphthyl)-3-[4-(4-nitro-2-trifluoromethylphenyl)piperazin-1-yl] propan-1-one (Compound **4**)* (17% Yield) Mp 182–183ºC. ^{1}H NMR (400 MHz, DMSO-d_6): δ 3.21 (d, 2H, **H_{2ax}**+**H_{6ax}** piperazine); 3.27 (d, 2H, **H_{2ec}**+**H_{6ec}** piperazine); 3.64 (bs, 2H, **H_{3ax}**+**H_{5ax}** piperazine); 3.67 (bs, 2H, **H_{3ec}**+**H_{5ec}** piperazine); 3.90 (t, 2H, CO-CH_2-**CH_2**); 4.03 (t, 2H, CO- **CH_2**); 7.65-7.59 (m, 3H, **H_6**+**H_7** naphthyl+**$H_{6'}$** phenyl); 7.92 (d, 1H, **H_4** naphthyl, $J_{4,3}$ = 7.9 Hz); 7.95 (d, 1H, **H_5** naphthyl, $J_{5,6}$ = 8.7 Hz); 8.04 (d, 1H, **H_8** naphthyl, $J_{8,7}$ = 8.3 Hz); 8.06 (d, 1H, **H_3** naphthyl, $J_{3,4}$ = 7.9 Hz); 8.46 (d-d, 1H, **$H_{5'}$** phenyl, $J_{5',6'}$ = 8.8 Hz, $J_{5',3'}$ = 2.5 Hz); 8.58 (d, 1H, **$H_{3'}$** phenyl, $J_{3',5'}$ = 2.5 Hz);

8.62 (bs, 1H, **H_1** naphthyl) ppm. Anal ($C_{24}H_{22}N_3F_3O_3$.2HCl) C, H, N.

*Hydrochloride of 1-(2-naphthyl)-3-[3-(4-nitro-2-trifluoromethylphenyl)-(S)-pyrrolidin-3-ylamino] propan-1-ona (Compound **5**)* (38% Yield). Mp 171-172 ºC. ^{1}H NMR (400 MHz, DMSO-d_6): δ 2.38 (d-d, 1H, **H_{4ec}** pyrrolidine); 2.45 (d-d, 1H, **H_{4ax}** pyrrolidine); 3.42 (d, 2H, CO-CH_2-**CH_2**); 3.64 (d-d, 1H, **H_{2ec}** pyrrolidine); 3.75 (t, 2H, CO-**CH_2**); 3.81- 3.86 (m, 2H, **H_{5ec}**+ **H_{2ax}** pyrrolidine); 3.94 (d-d, 1H, **H_{5ax}** pyrrolidine); 4.08 (bs, 1H, **H_3** pyrrolidine); 7.12 (d, 1H, **$H_{6'}$** phenyl, $J_{6',5'}$ = 9.6 Hz); 7.65 (d-d, 1H, **H_6** naphthyl, $J_{6,7}$ = 7.8 Hz, $J_{6,5}$ = 6.8 Hz); 7.69 (d-d, 1H, **H_7** naphthyl, $J_{7,6}$ = 7.8 Hz, $J_{7,8}$ = 8.35 Hz); 8.00 (d, 1H, **H_4** naphthyl, $J_{4,3}$ = 6.5 Hz); 8.02 (d, 1H, **H_3** naphthyl, $J_{3,4}$ = 6.5 Hz); 8.06 (d, 1H, **$H_{5'}$** phenyl, $J_{5',6'}$ = 8.6 Hz); 8.16 (d, 1H, **H_5** naphthyl, $J_{5,6}$ = 6.8 Hz); 8.25 (d,1H, **H_8** naphthyl, $J_{7,8}$ = 8.35 Hz); 8.39 (bs, 1H, **$H_{5'}$** phenyl); 8.69 (bs, 1H, **H_1** naphthyl); 9.80 (bs, 2H, NH+ClH) ppm. Anal ($C_{24}H_{22}N_3F_3O_3$.HCl) C, H, N.

*1-(4-fluoronaphthyl)-3-[4-(2-nitro-4-trifluoromethylphenyl)piperazin-1-yl]propan-1-one (Compound **6**)* (73% Yield). Mp 106–107ºC. ^{1}H NMR (400 MHz, $CDCl_3$): δ 2.70 (bs, 4H, **H_2**+**H_6** piperazine); 3.04 (bs, 2H, CO-CH_2-**CH_2**); 3.19 (bs, 4H, **H_3**+**H_5** piperazine); 3.35 (bs, 2H, CO-**CH_2**); 7.17 (d, 1H, **$H_{6'}$** phenyl, $J_{6',5'}$ = 8.8 Hz); 7.20 (d-d, 1H, **H_7** fluoronaphthyl, $J_{7,8}$ = 9.0 Hz, $J_{7,6}$ = 8.0 Hz); 7.63 (d-d-d, 1H, **H_6** fluoronaphthyl); 7.68 (d-d, 1H, **$H_{5'}$** phenyl, $J_{5',6'}$ = 8.8 Hz, $J_{5',3'}$ = 1.6 Hz); 7.69 (d-d, 1H, **H_5** fluoronaphthyl, $J_{5,6}$ = 7.3 Hz, J_{5F} = 2.7 Hz); 7.94 (d-d, 1H, **H_3** fluoronaphthyl, $J_{3,2}$ = 7.9 Hz, J_{3F} = 5.4 Hz); 8.07 (d, 1H, **$H_{3'}$** phenyl, $J_{3',5'}$ = 1.5 Hz); 8.19 (d, 1H, **H_2** fluoronaphthyl, $J_{2,3}$ = 7.9 Hz); 8.73 (d, 1H, **H_8** fluoronaphthyl, $J_{8,7}$ = 9.0 Hz) ppm. Anal ($C_{24}H_{21}N_3F_4O_3$) C, H, N.

*1-(benzo[b]thiophen-3-yl)-3-[4-(4-nitro-2-trifluoromethylphenyl)piperazin-1-yl]propan-1-ol (Compound **7**)* (30 % Yield). Mp 154-155ºC. ^{1}H NMR (400 MHz, $CDCl_3$): 2.14-2.16 (m, 2H, CHOH-C**H_2**); 2.77-2.87 (m, 6H, CHOH-CH_2-C**H_2** + **H_2**+**H_6** piperazine); 3.20-3.29 (m, 4H, **H_3**+ **H_5** piperazine); 5.38 (d-d, 1H, C**H**OH); 7.33-7.42 (m, 3H, **H_6**, phenyl + **H_6** + **H_5** benzothiophenyl); 7.45 (s, 1H, **H_2** benzothiophenyl); 7.82 (d, 1H, **H_4** benzothiophenyl, $J_{4,5}$ = 8.4 Hz); 7.88 (d, 1H, **H_7** benzothiophenyl, $J_{7,6}$ = 8.0 Hz); 8.37 (d-d, 1H, **H_5**, phenyl $J_{5',6'}$ = 9.2 Hz, $J_{5',3'}$ = 2.8 Hz); 8.55 (d, 1H, **H_3**, phenyl) ppm. Anal ($C_{22}H_{22}N_3F_3O_3S$) C, H, N.

*Hydrochloride of 1-(benzo[b]thiophen-3-yl)-3-[4-(2-nitro-4-trifluoromethylphenyl)piperazin-1-yl]propan-1-ol (Compound **8**)* (26% Yield). Mp 177–178ºC. ^{1}H NMR (400 MHz, DMSO-d_6): δ 2.23–2.32 (m, 2H, CHOH-**CH$_2$**); 3.17 (bs, 2H, CHOH-CH$_2$- **CH$_2$**); 3.35 (bs, 2H, **H$_{2ax}$**+**H$_{6ax}$** piperazine); 3.49 (bs, 4H, **H$_{3ax}$**+**H$_{5ax}$**+**H$_{2ec}$**+**H$_{6ec}$** piperazine); 3.59 (d, 2H, **H$_{3ec}$**+**H$_{5ec}$** piperazine); 5.01 (m, 1H, C**H**-OH); 7.43–7.36 (m, 2H, **H$_5$**+**H$_6$** benzothiophenyl); 7.54 (d, 1H, **H$_{6'}$** phenyl, $J_{6',5'}$ = 8.0 Hz); 7.64 (bs, 1H, H2 benzothiophenyl); 7.94 (d-d, 1H, **H$_{5'}$** phenyl, $J_{5',6'}$ = 8.8 Hz, $J_{5',3'}$ = 1.6 Hz); 7.98-8.01 (m, 2H, **H$_7$**+**H$_4$** benzothiophenyl); 8.25 (bs, 1H, **H$_{3'}$** phenyl); 11.11 (bs, 1H, **H**Cl) ppm. Anal ($C_{22}H_{22}N_3F_3O_3S$.HCl) C, H, N.

*Hydrochloride of 1-(2-naphthyl)-3-[4-(2-nitro-4-trifluoromethylphenyl)piperazin-1-yl]propan-1-ol (Compound **9**)* (63% Yield) Mp 185–186ºC. ^{1}H NMR (400 MHz, DMSO-d_6): δ 2.19-2.22 (m, 2H, CHOH-**CH$_2$**); 3.16 (bs, 2H, **H$_2$**+**H$_6$** piperazine); 3.48 (bs, 2H, **H$_3$**+**H$_5$** piperazine); 3.58 (d, 2H, CHOH-CH$_2$-**CH$_2$**); 4.84-4.87 (m, 1H, C**H**OH); 5.74 (bs, 1H, **OH**); 7.47-7.52 (m, 2H, **H$_{6'}$**phenyl+**H$_3$** naphthyl); 7.54 (bs, 1H, **H$_7$** naphthyl); 7.56 (bs, 1H, **H$_6$** naphthyl); 7.88-7.95 (m, 5H, **H$_1$**+**H$_5$**+**H$_8$**+**H$_4$** naphthyl+**H$_{5'}$** phenyl); 8.25 (bs, 1H, **H$_{3'}$** phenyl); 11.10 (bs, 1H, **H**Cl) ppm. Anal ($C_{24}H_{24}N_3F_3O_3$.HCl) C, H, N.

*Hydrochloride of 1-(2-naphthyl)-3-[3-(4-nitro-2-trifluoromethylphenyl)-(S)-pyrrolidin-3-ylamino] propan-1-ol (Compound **10**)* (20% Yield) Mp 181-183 ºC. ^{1}H NMR (400 MHz, DMSO-d_6): δ 2.07-2.14 (m, 2H, CHOH-C**H$_2$**); 2.29-2.31 (m, 1H, **H$_{4ec}$** pyrrolidine); 2.36-2.41 (m, 1H, **H$_{4ax}$** pyrrolidine); 3.11 (bs, 2H, CHOH-CH$_2$-C**H$_2$**); 3.57-3.64 (m, 1H, **H$_{2ec}$** pyrrolidine); 3.75-3.79 (m, 2H, **H$_{5ec}$**+ **H$_{2ax}$** pyrrolidine); 3.85-3.89 (m, 1H, **H$_{5ax}$** pyrrolidine); 3.97 (bs, 1H, **H$_3$** pyrrolidine); 5.90 (bs, 1H, C**H**OH); 5.76 (s, 1H, O**H**); 7.10 (d, 1H, **H$_{6'}$** phenyl, $J_{6',5'}$ = 9.6); 7.47-7.55 (m, 3H, **H$_3$** + **H$_6$** + **H$_7$** naphthyl); 7.86 (bs, 1H, **H$_1$** naphthyl); 7.90-7.92 (m, 3H, **H$_4$** + **H$_5$** + **H$_8$** naphthyl); 8.24-8.9 (d, 1H, **H$_{5'}$**, phenyl, $J_{5',6'}$ = 9.5); 8.40 (bs, 1H, **H$_{3'}$**, phenyl); 9.49 (bs, 1H, N**H**) ppm. Anal ($C_{24}H_{24}N_3F_3O_3$.HCl) C, H, N.

*1-(2-naphthyl)-2-[4-(2-nitro-4-trifluoromethylphenyl)piperazin-1-yl] ethan-1-ol (Compound **11**)* (78% Yield). Mp 133–134ºC. ^{1}H NMR (400 MHz, $CDCl_3$): δ 2.75-2.81 (m, 4H, **H$_2$**+**H$_6$** piperazine); 3.03 (bs, 2H, CHOH-**CH$_2$**); 3.26-3.31 (**H$_3$**+**H$_5$** piperazine); 5.04 (d-d, 1H, C**H**OH); 7.21 (d, 1H, **H$_{6'}$** phenyl, $J_{6',5'}$ = 8.7 Hz); 7.49-7.52 (m, 3H, **H$_3$**+**H$_6$**+**H$_7$** naphthyl); 7.71 (d-d, 1H, **H$_{5'}$** phenyl, $J_{5',6'}$ = 8.7 Hz, $J_{5',3'}$ = 1.9 Hz); 7.86 (bs,

1H, **H$_1$** naphthyl); 7.86 (d-d, 1H, **H$_8$** naphthyl, $J_{8,7}$ = 7.9 Hz, $J_{8,6}$ = 1.5 Hz); 7.88 (d, 1H, **H$_4$** naphthyl, $J_{4,3}$ = 5.5 Hz); 7.90 (bs, 1H, **H$_5$** naphthyl); 8.11 (d, 1H, **H$_{3'}$** phenyl, $J_{3',5'}$ = 1.9 Hz) ppm. Anal ($C_{23}H_{22}N_3F_3O_3$) C, H, N.

*1-(4-fluoronaphthyl)-3-[4-(2-nitro-4-trifluoromethylphenyl)piperazin-1-yl]propan-1-ol (Compound **12**)* (90% Yield) Mp 142–143ºC. ^{1}H NMR (400 MHz, $CDCl_3$): δ 2.08-2.18 (m, 2H, CHOH-CH_2); 2.83 (bs, 3H, **H$_5$** piperazine+ CHOH-CH_2-**C**$\mathbf{H_2}$); 2.95 (bs, 3H, **H$_3$** piperazine+ CHOH-CH_2-**C**$\mathbf{H_2}$); 3.32 (bs, 4H, **H$_2$**+**H$_6$** piperazine); 5.71 (d-d, 1H, C**H**OH); 7.18 (d-d, 1H, **H$_3$** fluoronaphthyl, J_{3F} = 10.2 Hz, $J_{3,2}$ = 8.1 Hz); 7.23 (d, 1H, **H$_{6'}$** phenyl, $J_{6',5'}$ = 8.7 Hz); 7.54-7.62 (m, 2H, **H$_6$**+**H$_7$** fluoronaphthyl); 7.68 (d-d, 1H, **H$_2$** fluoronaphthyl, $J_{2,3}$ = 8.0 Hz, J_{2F} = 5.6 Hz); 7.74 (d-d, 1H, **H$_{5'}$** phenyl, $J_{5',6'}$ = 8.7 Hz, $J_{5',3'}$ = 1.9 Hz); 8.05 (d-d, 1H, **H$_5$** fluoronaphthyl, $J_{5,6}$ = 8.2 Hz, J_{5F} = 1.7 Hz); 8.11 (d, 1H, **H$_{3'}$** phenyl, $J_{3',5'}$ = 1.9 Hz); 8.17 (d-d, 1H, **H$_8$** fluoronaphthyl, $J_{8,7}$ = 6.6 Hz, $J_{8,6}$ = 2.9 Hz) ppm. Anal ($C_{24}H_{23}N_3F_4O_3$) C, H, N.

*1-(4-fluoronaphthyl)-3-[4-(4-nitro-2-trifluoromethylphenyl)piperazin-1-yl]propan-1-ol (Compound **13**)* (22% Yield) Mp 183–184ºC. ^{1}H NMR (400 MHz, DMSO-d_6): δ 1.83-1.94 (m, 2H, CHOH-**C**$\mathbf{H_2}$); 2.49-2.51 (m, 4H, **H$_2$**+**H$_6$** piperazine); 2.54 (bs, 2H, CHOH-CH_2-**C**$\mathbf{H_2}$); 3.14-3.16 (m, 4H, **H$_3$**+**H$_5$** piperazine); 5.39-5.42 (m, 1H, C**H**OH); 7.31 (d, 1H, **H$_3$** fluoronaphthyl, J_{3F} = 10,7 Hz); 7.56 (d, 1H, **H$_{6'}$** phenyl, $J_{6',5'}$ = 8.5 Hz); 7.61-7.69 (m, 3H, **H$_6$**+**H$_7$**+**H$_2$** fluoronaphthyl); 8.08 (d-d, 1H, **H$_{5'}$** phenyl, $J_{5',6'}$ = 8.5 Hz, $J_{5',3'}$ = 1.4 Hz); 8.26 (d, 1H, **H$_8$** fluoronaphthyl, $J_{8,7}$ = 8.0 Hz); 8.38 (bs, 1H, **H$_{3'}$** phenyl); 8.39 (d-d, 1H, **H$_5$** fluoronaphthyl, $J_{5,6}$ = 12.0 Hz, J_{5F} = 2.7 Hz) ppm. Anal ($C_{24}H_{23}N_3F_4O_3$) C, H, N.

*1-(2-naphthyl)-3-[3-(4-nitro-2-trifluoromethylphenyl)-(S)-pyrrolidin-3-ylamino] propan-1-oxime (Compound **14**)* (45% Yield) Mp 130-131 ºC. ^{1}H NMR (400 MHz, DMSO-d_6): δ 1.78-1.85 (m, 1H, **H$_{4ax}$** pyrrolidine); 2.02-2.09 (m, 1H, **H$_{4ec}$** pyrrolidine); 2.21 (bs, 1H, -N**H**-); 2.70-2.82 (m, 2H, CN-CH_2-**C**$\mathbf{H_2}$-N); 3.00 (t, 2H, CN-**C**$\mathbf{H_2}$); 3.25 (dd, 1H, **H$_3$** pyrrolidine,); 3.43-3.51 (m, 2H, **H$_{2ax}$**+ **H$_{2ec}$** pyrrolidine); 3.60 (m, 2H, **H$_5$** pyrrolidine); 6.97 (d, 1H, , **H$_{6'}$** phenyl, $J_{6',5'}$ = 9.6 Hz); 7.51 (d, 1H, **H$_5$** naphthyl, $J_{5,6}$ = 6.1 Hz); 7.52 (d, 1H, **H$_8$** naphthyl, $J_{8,7}$ = 6.1 Hz); 7.86 (bs, 2H, **H$_3$**+**H$_4$** naphthyl); 7.88-7.94 (m, 2H, **H$_6$**+**H$_7$** naphthyl); 8.13 (bs, 1H, **H$_1$** naphthyl); 8.15 (dd, 1H, **H$_{5'}$** phenyl, $J_{5',6'}$ = 9.4 Hz, $J_{5',3'}$ = 2.7 Hz); 8.35 (d, 1H, **H$_{3'}$** phenyl, $J_{3',5'}$ = 2.7 Hz) ppm. Anal ($C_{24}H_{23}N_4F_3O_3$) C, H, N.

2.4. Biological tests

2.4.1. In vitro antiplasmodial drug assay

Culture of chloroquine resistant Colombian FCR-3 strain of *Plasmodium falciparum* was carried out at 37°C in 5% CO_2 environment on glucose-enriched RPMI 1640 medium supplemented with gentamycin 0.1mg/ml and 10% heat-inactivated human serum, as previously described (Trager and Jensen, 1976). The drugs, dissolved in dimethylsulfoxide (DMSO), were added at final concentrations ranging from 200 to 0,1µM. All experiments were performed in triplicate. The final DMSO concentration was never greater than 0.1%. *In vitro* antimalarial activity was measured using the [^{3}H]-hypoxanthine (MP Biomedicals, USA) incorporation assay (Desjardin et al., 1979). All experiments were performed in triplicate. Results were expressed as the Concentration resulting in 50% Inhibition (IC_{50}) ± Standard Deviation that was calculated by linear interpolation (Huber and Koella, 1993) as follow:

$\text{Log}(IC_{50}) = \log(X1) + (50-Y1)/(Y2-Y1)\,[\log(X2) - \log(X1)]$

X1: concentration of the drug that gives a %inhibition of the parasitaemia Y1>50%

X2: concentration of the drug that gives a %inhibition of the parasitaemia Y2<50%

% Inhibition of the incorporation of labelled hypoxanthine = 100 – (P/T * 100)

P: c.p.m. for every concentrations.

T: negative control (red blood cells without drug).

2.4.2. In vivo antiplasmodial drug assay

In vivo studies were conducted according to the French and Colombian legislations on laboratory animal use and care (N°2001-464 and N° 008430, respectively). The classical 4-day suppressive test (Peters and Robinson, 1999) was conducted with *P. berghei* ANKA. Swiss female mice (*Bioterio DFUNC*) weighing 20 ± 2 g, were infected with 10^7 parasitized cells in 0,9% saline solution (day 0). Two hours after being infected (same time for 4 consecutive days), batches of ten mice were orally treated with the most active compound at 10 mg/kg/day. A control group received 0,9% saline solution while a reference group received chloroquine diphosphate (CQ) at 5 mg/kg/day (oral route). Survival of the mice was checked daily and the percentage of parasitized erythrocytes was determined on day 4, for which purpose Giemsa-stained thin blood smears were made from peripheral blood. The percentage of inhibition of parasitaemia was calculated, and the ED_{50} was determined with a linear least square regression analysis.

2.4.3. Toxicity Assay

Toxicity was assessed on murine macrophages harvested from peritoneal cavities of 6-8 week-old female BALB/c mice in ice-cold M199 medium supplemented with 10 % FBS (Sauvain et al., 1993). Dilutions of drugs to be tested in complete medium were added to achieve a final volume of 100 µl from 200 to 0,1µM. The culture was continued for another 48 h. After that, the number of viable cells was scored by hematocytometer using 0.4 % trypan blue solution in PBS (adapted from Castillo et al., 2007). The half-maximal cytotoxic concentration 50 (CC_{50}) was determined. All experiments were repeated 3 times.

Cytotoxicity was also assessed, for the most active compound, on BALB/3T3 (Non-tumorogenic, BALB/c mouse embryo), Vero (African green monkey kidney), HT-29 (human colon adenocarcinoma), and K562 (human chronic myelogenous leukemia) cells. Briefly, the cells were incubated in 96-well plates with the most active compound for 48 hours at 37°C in a 5% CO_2 and 95 % air humidified atmosphere. The percent inhibition of cell growth relative to control was determined with sulforhodamine B dye according to Skehan, et al. (1990) and Boyd and Paull (1995), except for K562 cells, which grow in suspension, instead of fixing and staining with sulforhodamine B, cells were counted using a Coulter counter. The $GI_{50,}$ determined by linear regression analysis, was defined as the concentration of test sample resulting in a 50% reduction of absorbance as compared with controls.

2.5. Physicochemical Parameters Calculation.

Virtual Computational Chemistry Laboratory (http://www.vcclab.org/) (Tetko et al., 2005) and Molinspiration online property calculation toolkit (http://www.molinspiration.com/services/properties.html) were used to calculate Topological Polar Surface Area (Ertl, et al., 2000) miLog*P*, AlogPS2.1, KOWLogP, LogP (AB/logP), number of rotable bonds, and violations of Lipinski's rule of five (Lipinski *et al*., 1997). Absorption (%ABS) was calculated by: %ABS = 109 - (0.345 × TPSA). (Zhao *et al*., 2002).

2.6. Optimized Geometry and Molecular Electrostatic Potentials.

The complete geometry optimization of the active compound was performed using Quantum mechanics calculation. To achieve this goal ab initio quantum chemistry program Gaussian (Gaussian, Inc., Pittsburgh PA, 2003.) and the HF/3-21G basis set

were used. Molecular electrostatic potential (MEP) was computed from the electronic density and displayed using Molekel software (http://www.cscs.ch/molekel/) (Flükiger et al., 2008)

2.7. Computational docking Studies.

The molecular docking program Autodock 4.0 was used to determine the potential binding mode between the most active synthesized compound **13** and the selected *Plasmodium plasmepsin II* enzyme candidate target. Firstly, in order to validate our methodology and check the ability of the program Autodock to investigate the binding mode of inhibitors into the binding site of the enzyme, the complex *Plasmodium plasmepsin II* with EH58 (Asojo et al., 2003) was computational re-docked (PDB code 1LF3). As reported Cunico *et al*. (2009a,b), RMSD values up to 3.0 Å were considered correctly docked structures (see table 4). To prepare the input structures for Autodock calculations (Morris et al., 1998), the structure of *Plasmodium plasmepsin II* was used as candidate target. According to previous study (Cunico et al. 2009b), the residues involved in the active site were treated as follows: Asp34 (OD1) was held protonated while Asp214 was negatively charged; protein was further manipulated by adding Kollman partial charges and solvent parameters. Similarly to the protein, the structure of the compound **13** was also prepared by deleting their non-polar hydrogen atoms and adding Mulliken atomic charges obtained from Gaussian03.

The Lamarckian Genetic Algorithm (LGA) implemented in the Autodock program was applied following a protocol of 10 independent runs with a population size of 150 individuals, a maximum number of $2.5x10^7$ energy evaluations, a mutation rate of 0.02, a crossover rate of 0.80 and an elitism value of 1. These parameters were sufficient for the objective of a first approach for target search.

The most representative binding modes of the ten conformations calculated, with at least one hydrogen bond with one of the catalytic aspartates, were chosen for analysis (Kasam et al., 2007; Åqvist et al., 1994). The binding energies and RMSD values of EH58 and the binding energies of compound **13** for the ten docked conformations are shown in Table 4.

3. Results and discussion

Fourteen new compounds (1-aryl-ketone, 1-aryl-alcohol and 1-aryl-oxime derivatives) were evaluated against *P. falciparum* and murine macrophage: (see table 1).

As expected (Pérez Silanes et al., 2009), none of the aryl-ketones (compounds **1-6**)

were considered active on malaria parasite, being 100-450 times less active than chloroquine (IC_{50}: 0.4μM). Similarly, the only aryl-oxime tested (compound **14**) was also almost 100 times less active than chloroquine. The most interesting compounds (**7**, **8, 10**, **12** and **13**) were found among the aryl-alcohol derivatives. This fact confirms that the OH group present in the propane chain is essential for the activity (see compounds **7** vs **1**, **10** vs **5** and **12** vs **6**).

Interestingly, when the position of the nitro and trifluromethyl phenyl groups were swapped (see compounds **12** vs **13** and **7** vs **8**), the activity changed, reaching up to 10 times higher in the case of the most active compound: **13** (IC50: 0.5 μM similar to that of the control drug, chloroquine). In all cases, the scaffold 4-nitro-2-trifluoromethyl phenyl was the most interesting.

Shortening the carbon chain (ethane instead of propane) leads to a large decrease of the activity (see compound **11** vs **9** and **2** vs **4**). This was also the case in Ar' when the 4-fluoro-1-naphtyl was replaced by Benzo[b]thiophenyl or by 2-naphthyl (see **12** vs **8** vs **9**), the activity dropping drastically in this order.

With regard to the toxicity on murine peritoneal macrophages, compounds **2, 3** and **13** were the less cytotoxic of the tested series. On the contrary, **6** and **14** were the most toxic compounds, being 10 times more toxic than compound **2, 3, 9** and **13**. The most active compounds **7**, **8, 10, 12** and **13** (1-aryl-alcohol derivatives) showed different cytotoxicity on murine macrophages. No clear, evident relationship could be established between the structure of the compounds and the toxicity shown. Compound **13** had the best safety/activity on murine macrophages, rate being even better than chloroquine the later was almost 150 times more active than toxic. Regarding its toxicity against cells in replication: it inhibited 50% of cells growth at 10,2 μM for BALB/3T3 (Non-tumorogenic, BALB/c mouse embryo), 20,9 μM for Vero (African green monkey kidney), 15,4 μM for HT-29 (human colon adenocarcinoma), and 15,8 μM for K562 (human chronic myelogenous leukemia) cells. It was then almost 20-40 times more active against *Plasmodium* than against those cells (table 2). The convergence of good activity against *P. falciparum*, low cytotoxicity and favourable physico-chemical properties (see below), prompted us to test this compound against *P. berghei* murine malaria. Unfortunately the compound was hardly soluble in classically used solvents for oral administration. This may explain why it inhibited only 35% of parasite growth while chloroquine cleared parasite at a two times lower dose.

In a physico-chemical perspective (table 3), all of the compounds respected Lipinski's rules, as they all have a molecular weight under 500 Daltons, a limited lipophilicity

(expressed by Log P < 5, with P = [drug]org./[drug]aq.), far less than 5 H-bond donors (expressed as the sum of OHs and NHs), and also far less than 10 H-bond acceptors (expressed as the sum of Os and Ns). The series also presented a high % ABS, all of the compounds being potentially able to cross biological membranes.

In the search of a potential target and interactions responsible for biological activity to compound **13**, geometric optimization, molecular electrostatic potential (MEP) and computational molecular binding studies were carried out. MEP was generated for compound **13** after its geometry was energy-minimized (see methodology). As we expected, calculated potentials using ab initio method, showed a net electronegative potential around piperazine group and partial electronegative potentials around fluor, hydroxyl and nitro groups (fig.4.a.b.). From which is inferred that the most active compounds (1-aryl-alcohol derivatives), would share a similar distribution of electronegative potential and mode of action. Computational docking study was then performed between plasmepsin II and compound **13**. We found that this compound made an hydrogen bond with one of the catalytic aspartates on the active site of the enzyme (Asp214 and Asp34). This interaction involves the unique hydroxyl group present in the compound **13** and the residue Asp214 (fig.5a.). Besides, it provides us a possible rational explanation of the vital role of hydroxyl group to modulate the activity of the compound **13** and aryl derivates. In fact, as it has previously been reported, this interaction is mandatory in inhibitors of plasmepsin II (Bjelic et al., 2007). This mode of union is associated with a free gibbs energy of -6.16 Kcal/mol with a theoretical Ki of 30.6 uM which is superior than other values of free energy to piperazine derivatives (Cunico et al., 2009b). It is also reflected in the IC50 value reported for this compound by our results *in vitro*. Molecular docking studies also suggested subsites of union to compound **13**, situated near to the S1', S1 and S3 pocket of the protein (fig.5b). The 4-nitro-2-trifluromethyl phenyl group of this conformation was set near the S1 and S3 pocket and the 4-fluoro-1-naphtyl is located in the vicinity of the S2 pocket.

In conclusion, the most interesting compound was **13** 1-(4-fluoronaphthyl)-3-[4-(4-nitro-2-trifluoromethylphenyl) piperazin-1-yl]propan-1-ol. Further investigations are warranted to explore its *in vivo* antimalarial activity against murine malaria parasite with a new galenic form in order to enhance its solubility and to confirm that it really targets plasmodial plasmepsin II (Dell'Agli et al., 2009).

Acknowledgements

This work was support by PiUNA.

The authors gratefully acknowledge the financial assistance of the "Oficina de Cooperación de la Embajada de Bélgica" for funding the studies of Germán González, and the University of Navarra (Spain) for PhD scholarship supported to Adela Mendoza.

We also thank Ms Marie-Jean Manrique for the critical reading of this manuscript.

References

Åqvist, J., Medina, C., Samuelsson, J.E., 1994. A new method for predicting binding affinity in computer-aided drug design. Prot. Eng. 7, 385-391.

Asojo, O.A., Gulnik, S.V., Afonina, E., Yu, B., Ellman, J.A., Haque, T.S., Silva, A.M. 2003. Novel uncomplexed and complexed structures of plasmepsin II, an aspartic protease from *Plasmodium falciparum*. J. Mol. Biol. 327, 173-181.

Bjelic, S., Nervall, M., Gutiérrez-de-Terán, H., Ersmark, K., Hallberg, A., Åqvist, J. 2007. Computational inhibitor design against malaria plasmepsins. Cell. Mol. Life Sci. 64, 2285-2305.

Boyd, M.R., Paull, K.D., 1995. Some practical considerations and applications of the National Cancer Institute *in vitro* anticancer drug discovery screen. Drug Development Research. 34, 91-109.

Bruckner, R., 2002. Advanced organic chemistry: reaction mechanisms. San Diego: Harcourt/Academic Press, cop. 636pp.

Castillo, D., Arevalo, J., Herrera, F., Ruiz, C., Rojas, R., Rengifo, E., Vaisberg, A., Lock, O., Lemesre, J. L., Gornitzka, H., Sauvain, M., 2007. Spirolactone iridoids might be responsible for the antileishmanial activity of a Peruvian traditional remedy made with *Himatanthus sucuuba* (Apocynaceae). Journal of Ethnopharmacology 112, 410-414.

Cunico W., Gomes, C.R., Facchinetti, V., Moreth, M, Penido, C, Henriques, MG,

Varotti, F.P., Krettli, L.G., Krettli, AU, da Silva, F.S., Caffarena, E.R., de Magalhães, C.S., 2009. Synthesis, antimalarial evaluation and molecular modeling studies of hydroxyethylpiperazines, potential aspartyl protease inhibitors, part 2. European Journal of Medicinal Chemistry 44, 3816-3820.

Cunico, W., Gomes, C.R., Moreth, M., Manhanini, D.P., Figueiredo, I.H., Penido, C., Henriques, M.G., Varotti, F.P., Krettli, A.U., 2009. Synthesis and antimalarial activity of hydroxyethylpiperazine derivatives. European Journal of Medicinal Chemistry 44, 1363-1368.

Dell'Agli, M., Galli, G.V., Corbett, Y., Taramelli, D., Lucantoni, L., Habluetzel, A., Maschi, O., Caruso, D., Giavarini, F., Romeo, S., Bhattacharya, D., Bosisio, E., 2009. Antiplasmodial activity of *Punica granatum* L. fruit rind. Journal of Ethnopharmacology. 125, 279-285.

Desjardins, R.E., Canfield, C.J., Haynes, J.D., Chulay, J.D., 1979. Quantitative assessment of antimalarial activity *in vitro* by semiautomated microdilution technique. Antimicrobial Agents and Chemotherapy 16, 710-718.

Ersmark, K., Samuelsson, B., Hallberg, A. 2006. Plasmepsins as potential targets for new antimalarial therapy. Med Res Rev. 26, 626-666.

Ertl, P., Rohde, B., Selzer, P., 2000. Fast calculation of molecular polar surface area as a sum of fragment based contributions and its application to the prediction of drug transport properties. Journal of Medicinal Chemistry 43, 3714–3717.

Fautz, R., Husein, B., Hechenberger, C., 1991. Application of the neutral red assay (NR assay) to monolayer cultures of primary hepatocytes: rapid colorimetric viability determination for the unscheduled DNA synthesis test (UDS). Mutation Research 253, 173-179.

Flükiger, P., Lüthi, H. P., Portmann, J., Weber, S., 2008. MOLEKEL 5.3, Swiss Center for Scientific Computing, Manno (Switzerland).

Huber, W., and Koella, J.C., 1993. A comparison of three methods of estimating EC50 in studies of drug resistance of malaria parasites. Acta Tropica 55, 257-261.

Kasam, V., Zimmermann, M., Maass, A., Schwichtenberg H, Wolf A, Jacq N, Breton V, Hofmann-Apitius M. 2007. Design of new plasmepsin inhibitors: a virtual high throughput screening approach on the EGEE grid. J Chem Inf Model. 47(5):1818-28.

Lipinski, C.A., Lombardo, F., Dominy, B.W., Feeney, P.J., 1997. Experimental and computational approaches to estimate solubility and permeability in drug discovery and development settings. Advanced Drug Delivery Reviews 23, 3–25.

Morris GM, Goodsell DS, Halliday RS, Huey R, Hart WE, Belew RK, Olson, A. J. J. 1998 Automated docking using a Lamarckian genetic algorithm and empirical binding free energy function. J Comp Chem; 19: 1639-62

Oficialdegui, A., Martínez Esparza, J., Pérez Silanes, S., Heras, B., Irurzun, M., Palop, J.A., Monge, A., 2000. Design, synthesis and biological evaluation of new 3-[(4-aryl)piperazin-1-yl]-1-aryl propane derivatives as potential antidepressants with a dual mode of action: serotonin reuptake inhibition and 5-HT_{1A} receptor antagonism. Farmaco 55, 345-353.

Pérez-Silanes, L., Berrade, R.N., García–Sánchez, A., Mendoza, S., Galiano, B., Martín-P.Solórzano, J.J., Nogal-Ruiz, A.R., Martínez-Fernández, I., Aldana, Monge. A., 2009. New 1-aryl-3-substituted propanol derivatives as antimalarial agents. Molecules 14, 4120- 4135.

Peters W, Robinson BL. Handbook of animal models of infection. New York: Academic Press;1999.

Sauvain, M., Dedet, J.P., Kunesch, N., Poisson, J., Gayral, P., Gantier, J.C., Kunesch, G., 1993. *In vitro* and *in vivo* leishmanicidal activities of natural and synthetic quinoids". Phytotherapy Research 7, 167-171.

Trager, W., Jensen, J.B., 1976. Human malaria in continuous culture. Science 193, 673-675.

Skehan, P., Storeng, R., Scudiero, D., Monks, A., McMahon, J., Vistica, D., Warren, J,

Bokesch, H., Kenney, S., Boyd, M., 1990. New colorimetric cytotoxicity assay for anticancer-drug screening. Journal of the National Cancer Institute. 82, 1107-1112.

Tetko, I.V., Gasteiger, J., Todeschini, R., Mauri, A., Livingstone, D., Ertl, P., Palyulin, V.A., Radchenko, E.V., Zefirov, N.S., Makarenko, A.S., Tanchuk, V.Y., Prokopenko, V.V., 2005. Virtual computational chemistry laboratory - design and description, J. Comput. Aid. Mol. Des. 19, 453-463.

WHO. 2008. World Malaria Report. Geneva, World Health Organization. http://rbm.who.int/wmr.2008

Zhao, Y., Abraham, M.H., Lee, J., Hersey, A., Luscombe, N.C., Beck, G., Sherborne, B., Cooper, I. 2002. Rate-limited steps of human oral absorption and QSAR studies. Pharmaceutical Research 19, 1446–1457.

Figure 1. General mechanism of synthesis.

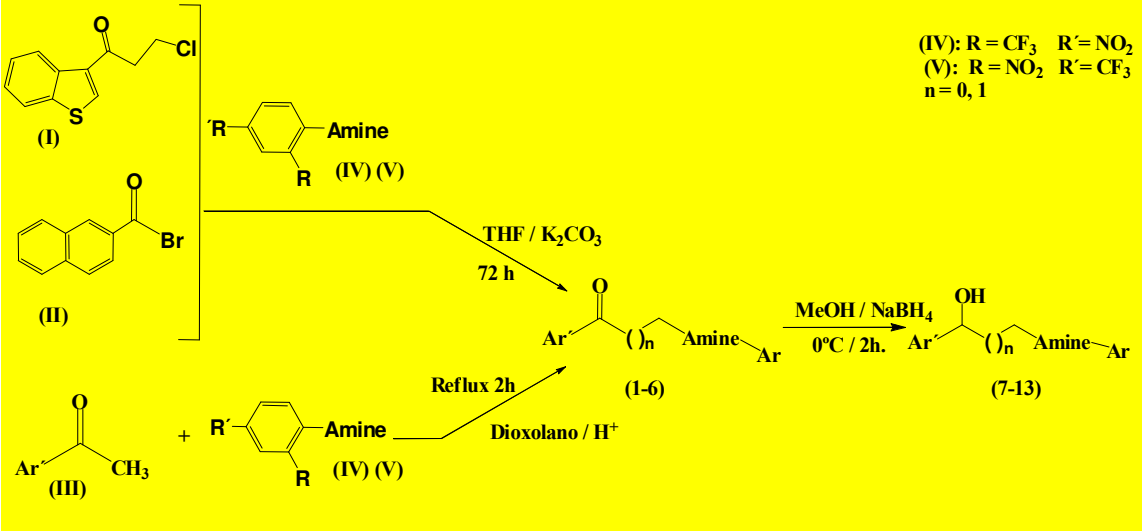

Figure 2. Synthesis of the arylamines not commercially available.

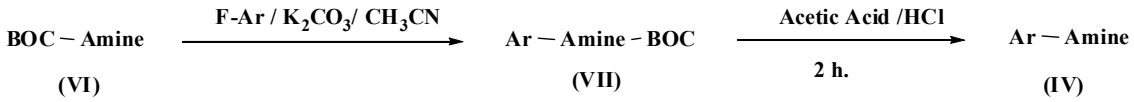

Figure 3. Synthesis of oxime derivative (**14**).

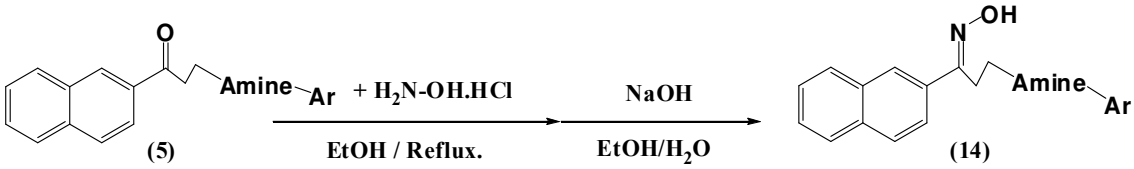

Figure 4.

Structure and molecular electrostatic potential (MEP) of the energy minimized structure of **13** (1- (4- fluoronaphthalen-1-yl)- 3– [4–(4-nitro -2-trifluoromethylphenyl) piperazin-1–yl] propanl – 1- ol). Negative potentials are in red while positive potentials are depicted in blue.

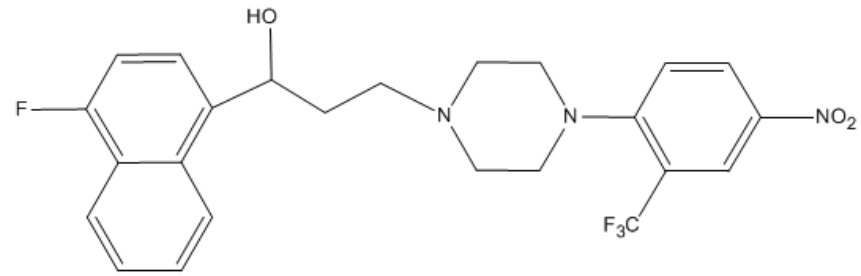

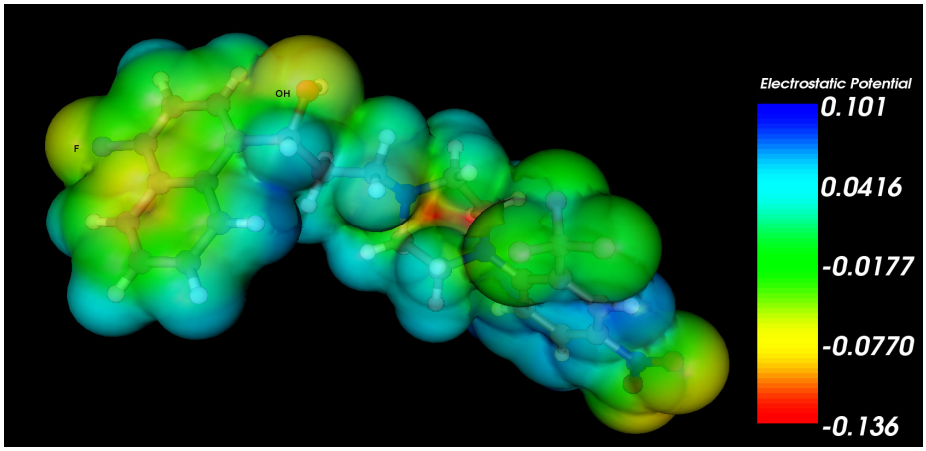

Figure 5. Main interaction and subsites of union between compound **13** (green) and active site of plasmepsin II.

a) Representation of the best conformation found for compound 13 within the active site of plasmepsin II. Hydrogen bond interaction (involving the hydroxyl group and Asp214) is coded by yellow dashed lines. Displayed in sticks only few residues with close contact.

b) Representative Molecular surface area of the complex plasmepsin II and compound 13. The flap loop region is represented by lines and dots involving residues 76-80. The subsites of the receptor are coloured, with S1 and S3 in purpleblue, S2 in magenta, S1' in orange and S2' in red. Residues of the active sites Asp214 and Asp34 are represented in sticks and coloured in blue

a

b

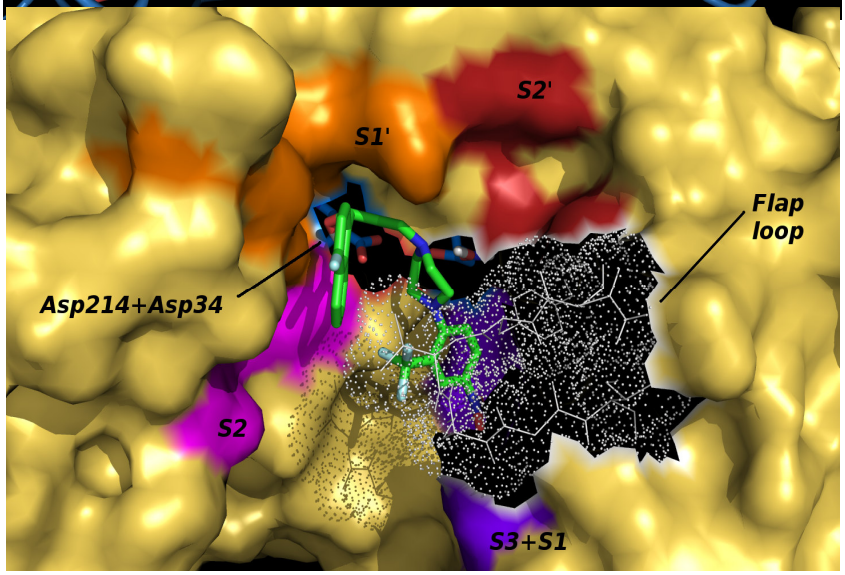

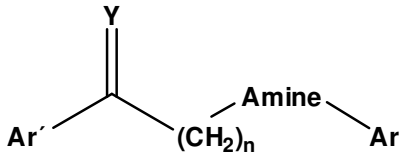

Comp.	Y	Ar´	n	Amine	Ar	IC_{50}	CC_{50}
1	C=O	Benzo[b]thiophenyl	2	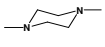	4-nitro-2-triflurometh yl phenyl	103.1	35.7
2	C=O	2-naphthyl	1	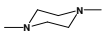	4-nitro-2-triflurometh yl phenyl	181.5	>100
3	C=O	2-naphthyl	1	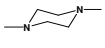	2-nitro-4-trifluorometil phenyl	172.3	>100
4	C=O	2-naphthyl	2	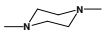	4-nitro-2-triflurometh yl phenyl	42.0	18.8
5	C=O	2-naphthyl	2	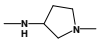	4-nitro-2-triflurometh yl phenyl	46.0	70.5
6	C=O	4-fluoro-1-naphtyl	2	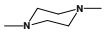	2-nitro-4-trifluorometil phenyl	73.0	9.6
7	CHOH	Benzo[b]thiophenyl	2	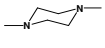	4-nitro-2-triflurometh yl phenyl	4.0	24.2
8	CHOH	Benzo[b]thiophenyl	2	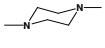	2-nitro-4-trifluorometil phenyl	10.3	36
9	CHOH	2-naphthyl	2	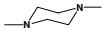	2-nitro-4-trifluorometil phenyl	52.6	98
10	CHOH	2-naphthyl	2	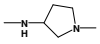	4-nitro-2-triflurometh yl phenyl	10.5	29.7
11	CHOH	2-naphthyl	1	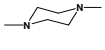	2-nitro-4-trifluorometil phenyl	102.2	74.7
12	CHOH	4-fluoro-1-naphtyl	2	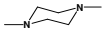	2-nitro-4-trifluorometil phenyl	4.9	75.6
13	CHOH	4-fluoro-1-naphtyl	2	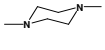	4-nitro-2-triflurometh yl phenyl	0.5	>100
14	C=NOH	2-naphthyl	2	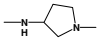	4-nitro-2-triflurometh yl phenyl	46.0	88
CQ						0.4	58

Table 1: *In vitro* antimalarial activity of tested compounds against FCR-3 Strain of *Plasmodium falciparum* and on *ex-vivo* murine macrophage. CQ: Chloroquine. ND: not determined (quitar esto) IC_{50} values represent the average of three determinations (determination of three independent experiments) and they are expressed in µM and represent inhibition of 50% of FCR-3 Strain of *Plasmodium* growth (IC_{50}) or *ex-vivo* murine macrophage survival (CC_{50}). Errors for individual measurements differed by less than 50%.

Table 2: comparative biological activities of compound **13** *in vitro* and *in vivo*.

cells	Activity μM
P. falciparum	0.5
Macrophage	>100
BALB/3T3	10.2
Vero	20.9
HT-29	15.4
K562	15.8
P. berghei	35% at 10mg/Kg

ID	%ABS	TPSA (Å^2)	*n*-ROTB	molecular weight	miLog*P*	KOWLogP	ALogPS 2.1	LogP (AB/logP)	MLogP	*n*-OHNH donors	*n*-ON acceptors	Lipinski's violations
rule				<500	<5	<5	<5	<5	<4.15	<5	<10	≤1
1	85.1	69.4	7	463.5	5.03	4.86	4.80	6.00	4.14	0	6	1
2	85.1	69.4	6	443.4	5.05	5.31	4.58	5.03	4.27	0	6	1
3	85.1	69.4	6	443.4	5.05	5.31	4.61	5.28	4.27	0	6	1
4	85.1	69.4	7	457.5	5.32	5.04	4.79	5.88	4.48	0	6	1
5	82.0	78.2	8	457.5	5.33	5.25	4.35	5.98	4.48	1	6	1
6	85.1	69.4	7	475.4	5.41	5.24	4.58	6.25	4.58	0	6	1
7	84.0	72.5	7	465.5	4.69	4.68	4.63	4.32	3.95	1	6	0
8	84.0	72.5	7	465.5	4.69	4.58	4.63	4.58	3.95	1	6	0
10	80.9	81.3	8	459.5	4.99	5.07	4.32	5.00	4.29	2	6	0
12	84.0	72.5	7	477.5	5.07	5.06	4.51	4.96	4.66	1	6	1
11	84.0	72.5	6	445.4	4.71	4.15	4.31	5.02	4.08	1	6	0
9	84.0	72.5	7	459.5	4.98	4.86	4.65	4.92	4.29	1	6	0
13	84.0	72.5	7	477.5	5.07	5.06	4.58	4.71	4.66	1	6	1
14	76.7	93.7	8	472.5	5.39	6.00	4.37	4.63	4.53	2	7	1
CQ	99.3	28.2	8	319.9	5.01	4.50	5.28	5.19	3.52	1	3	1

Table 3. Physical chemical properties of tested compounds

%ABS, percentage of absorption, calculated by: %ABS = 109 – (0.345 x TPSA), TPSA, topological polar surface area, *n*-ROTB, number of rotatable bonds, Log*P*, logarithm of compound partition coefficient between n-octanol and water, *n*-OHNH, number of hydrogen bond donors, *n*-ON, number of hydrogen bond acceptors. CQ: chloroquine.

Table 4. Compared molecular Docking Results between EH58 (as reported by Cunico et al., 2009b) and compound **13**.

	Compound EH58		Compound 13
Conf.[a]	Energy[b]	RMSD[c]	Energy[b]
1	-4.06	4.53	-6.16
2	-2.50	3.61	-6.07
3	-2.45	5.59	-5.85
4	-2.30	3.93	-5.84
5	-2.32	2.99	-5.70
6	-2.32	6.32	-5.56
7	-2.09	5.51	-5.56
8	-1.97	5.57	-5.45
9	-1.62	5.56	-5.25
10	-1.21	7.33	-4.78

[a] Best docking conformations sorted by energy ; [b] Autodock binding energy in kcal/mol; [c] RMSD values in Å.